Studying the $^3P_0$ decay model from QCD in Landau gauge

R. Alkofer, F.J. Llanes-Estrada & A. Salas-Bernárdez[†]

Univ. Complutense de Madrid (FJLE, ASB) & Univ. of Graz (RA)

Based on : Phys.Rev.D 109 (2024) 7, 074015

Present and future perspectives in Hadron Physics
INFN Frascati, 17/06/2024

Hadron decay and String Breaking

Usual picture for hadron decay:

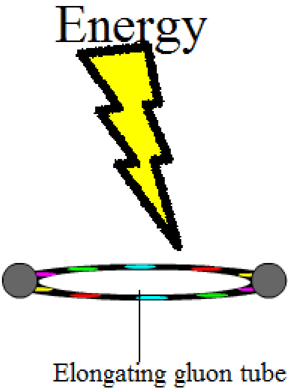

Hadron decay and String Breaking

Usual picture for hadron decay:

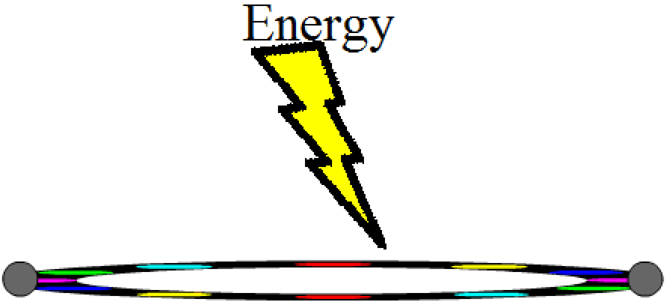

flux tube energy grows with inter-quark separation and creates a $q\bar{q}$ breaking the tube.

Usual picture for hadron decay:

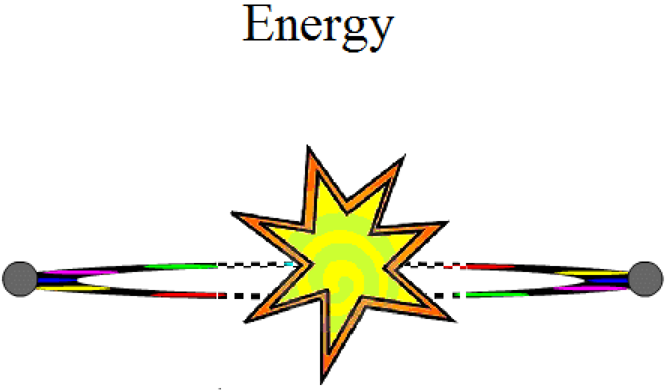

flux tube energy grows with inter-quark separation and creates a $q\bar{q}$ breaking the tube.

Hadron decay and String Breaking

Usual picture for hadron decay:

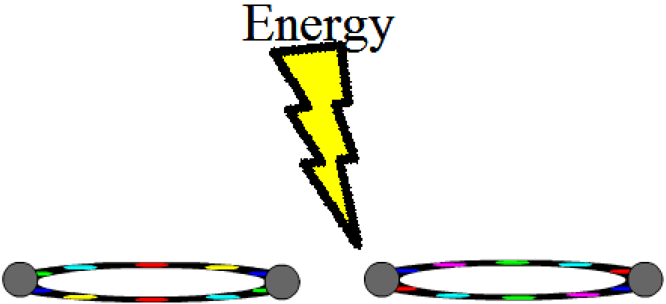

flux tube energy grows with inter-quark separation and creates a $q\bar{q}$ breaking the tube.

$q\bar{q}$ OZI-allowed meson decays

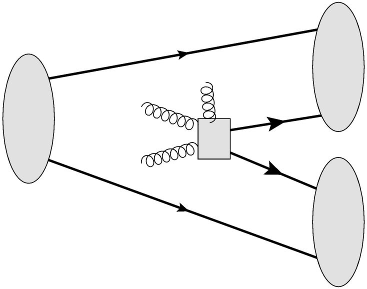

L. Micu, NPB 10 (1969) 521-526

$q\bar{q}$ OZI-allowed meson decays

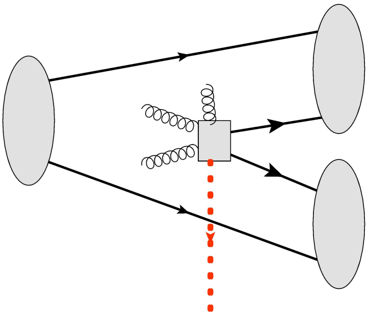

$$^1S_0, ^1P_1, ^3S_1, ^3P_0, ^3P_1, ^3P_2 \ldots ^{2S+1}L_J$$

Possible Q# of produced pair

L. Micu, NPB 10 (1969) 521-526

$q\bar{q}$ OZI-allowed meson decays

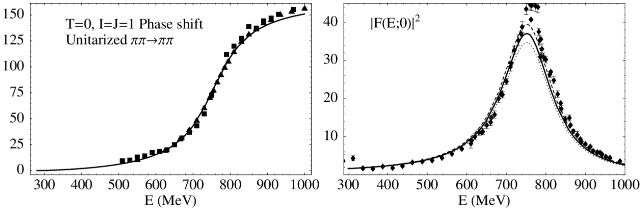

$$\cancel{{}^1S_0}, \cancel{{}^1P_1}, {}^3S_1, {}^3P_0, {}^3P_1, {}^3P_2 \dots$$

Think of $\rho(\uparrow\uparrow) \to \pi(\uparrow\downarrow)\pi(\uparrow\downarrow)$

A. Gómez-Nicola *et al.* PLB **606** 351-360 (2005)

$q\bar{q}$ OZI-allowed meson decays

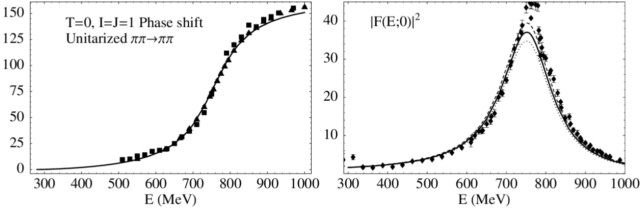

$${}^1S_0, {}^1P_1, \cancel{{}^3S_1}, {}^3P_0, {}^3P_1, {}^3P_2 \ldots$$

$$\text{Think of } \rho(\text{s-wave}) \to \underbrace{\pi(\text{s-wave})\pi(\text{s-wave})}_{L=1}$$

Transition amplitude must carry a P wave.

A. Gómez-Nicola *et al.* PLB **606** 351-360 (2005)

$q\bar{q}$ OZI-allowed meson decays

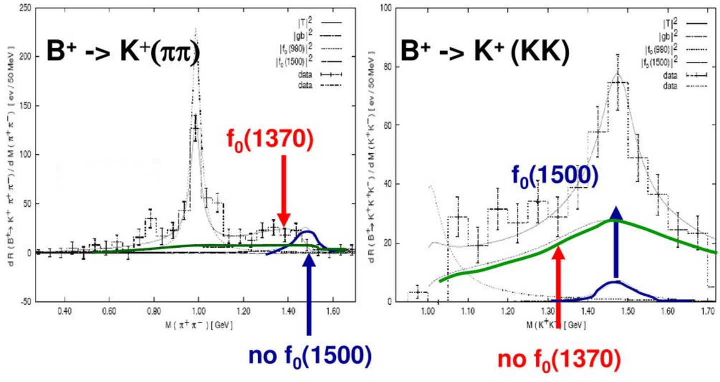

$$^1S_0, {}^1P_1, {}^3S_1, {}^3P_0, {}^3P_1, {}^3P_2 \dots$$

Move on to $\underbrace{f_0}_{\text{mainly } ^3P_0} \rightarrow \underbrace{\pi\pi}_{J=0}$

E. Klempt `https://slideplayer.com/slide/14648261/`

Lore: important $^3P_0$ pair production mechanism

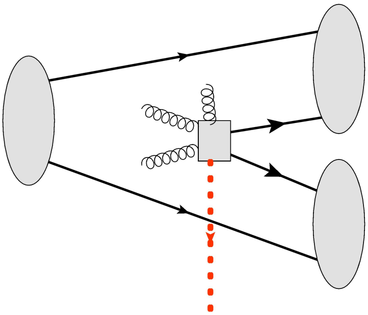

$^1S_0, ^1P_1, ^3S_1, ^3P_0, ^3P_1, ^3P_2 \ldots ^{2S+1}L_J$

Possible Q# of produced pair

L. Micu, NPB 10 (1969) 521-526

Not visible in QCD (or QED)

- $\int d^3x\ \bar{\psi}\ \boldsymbol{\gamma}\cdot\mathbf{A}\ \psi$ seems ${}^3S_1$

Not visible in QCD (or QED)

- $\int d^3x \; \bar{\psi} \; \boldsymbol{\gamma}\cdot\mathbf{A} \; \psi$ seems ${}^3S_1$
- Chiral-symmetry respecting at all orders in perturbation theory

Not visible in QCD (or QED)

- $\int d^3x\ \bar{\psi}\ \boldsymbol{\gamma}\cdot\mathbf{A}\ \psi$ seems $^3S_1$
- Chiral-symmetry respecting at all orders in perturbation theory
- But $^3P_0$ breaks chiral symmetry

Modelling the D/D_s spectrum with $^3P_0$: 32 modes studied by Close and Swanson

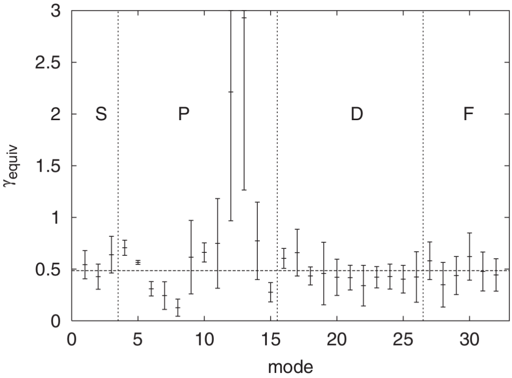

F. Close and E.S.Swanson PRD**72** 094004 (2005)

Effective Hamiltonian

$$H_{^3P_0} = \sqrt{3} g_s \int d^3\boldsymbol{x} \bar{\psi}(\boldsymbol{x}) \psi(\boldsymbol{x})$$

$\gamma = \frac{g_s}{2m}$

Effective Hamiltonian

$$H_{^3P_0} = \sqrt{3} g_s \int d^3\boldsymbol{x} \bar{\psi}(\boldsymbol{x}) \psi(\boldsymbol{x})$$

$\gamma = \frac{g_s}{2m}$

Chiral-symmetry breaking:

$$[Q_5, H_{^3P_0}] = \left[\int d^3\boldsymbol{x} \psi^\dagger(\boldsymbol{x}) \gamma_5 \psi(\boldsymbol{x}), H_{^3P_0} \right] \neq 0$$

Effective Hamiltonian

$$H_{^3P_0} = \sqrt{3} g_s \int d^3\boldsymbol{x} \bar{\psi}(\boldsymbol{x})\psi(\boldsymbol{x})$$

$\gamma = \frac{g_s}{2m}$

Chiral-symmetry breaking:

$$[Q_5, H_{^3P_0}] = \left[\int d^3\boldsymbol{x} \psi^\dagger(\boldsymbol{x})\gamma_5\psi(\boldsymbol{x}), H_{^3P_0}\right] \neq 0$$

$$i(2\pi)^4\delta^{(4)}(p+q)\mathcal{M}^{ss'}_{^3P_0}(p,q) = \langle \boldsymbol{p}s, \boldsymbol{q}s'|iT_{^3P_0}|0\rangle =$$
$$= (i\,(2\pi)^4\delta^{(4)}(p+q))(-\sqrt{3}g_s)\bar{u}^s(p)v^{s'}(q)$$

$$\boxed{\Rightarrow \bar{u}^s(\boldsymbol{p})v^{s'}(-\boldsymbol{p}) = 2\boldsymbol{p}\cdot\boldsymbol{\sigma}^{ss'}}$$

Dependence on the quark mass by Salamanca group

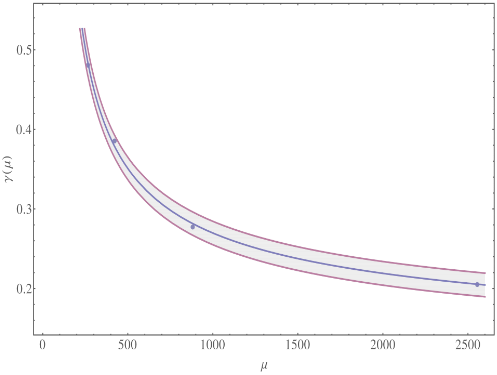

J. Segovia, D. R. Entem, F. Fernández Phys.Lett.B **715** (2012) 322-327

Dependence on the quark mass by Salamanca group

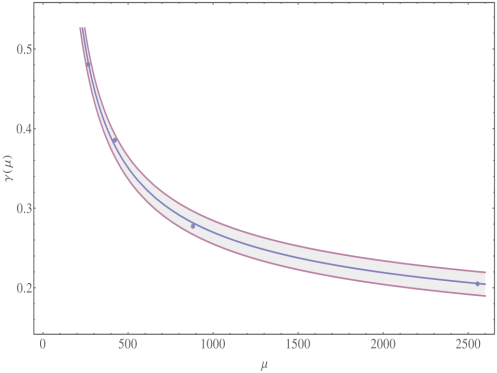

J. Segovia, D. R. Entem, F. Fernández Phys.Lett.B **715** (2012) 322-327

Recent work pointing towards the direction that this sub-process may also have a measurable impact on hadron structure: 2406.05920 M. Karliner and J.L. Rosner.

Our work: connect Quark-model pheno w. Landau gauge QCD

Can we obtain the $^3P_0$ effective Hamiltonian from *ab initio* QCD calculations?

Our work: connect Quark-model pheno w. Landau gauge QCD

Can we obtain the $^3P_0$ effective Hamiltonian from *ab initio* QCD calculations?

- N-gluon to $\bar{q}q$ kernel not known from first principles
- What to do with the information at hand?

Strategy: couple dynamical quarks to the flux tube background

Flux tube $\longleftrightarrow$ Dynamical quarks

Strategy: couple dynamical quarks to the flux tube background

Flux tube $\longleftrightarrow$ Dynamical quarks

Through Landau-gauge DSE primitive QCD Green's functions

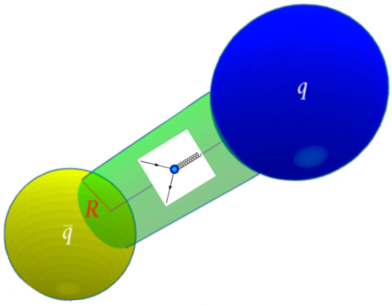

Extensive lattice+DSE work on Landau gauge primitive Green's functions

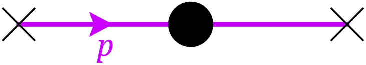

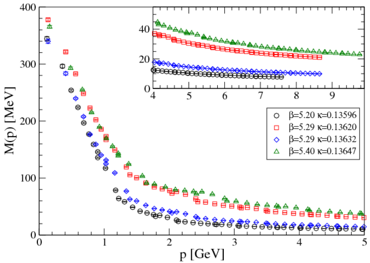

Lattice data from O. Oliveira *et al.* Acta Phys.Polon.Supp. 9 (2016) 363-368

Extensive lattice+DSE work on Landau gauge primitive Green's functions

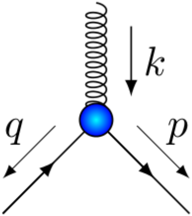

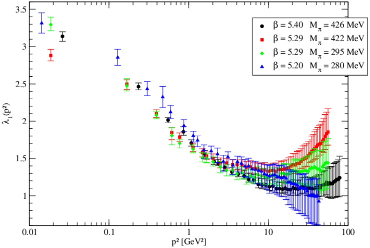

And also the pure Yang-Mills primitive Green's functions...

Lattice data from O. Oliveira *et al.* Acta Phys.Polon.Supp. 9 (2016) 363-368

Quark-Gluon vertex spin structure

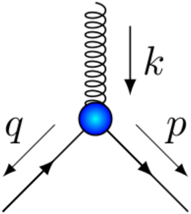

$$\Gamma^{\mu}_{T}(q_E, p_E; k_E) = \sum_{i=1}^{8} g_i(\bar{p}_E^2)\rho_i^{\mu}(q_E, p_E)$$

$$k^{\mu} = p^{\mu} + q^{\mu}$$

- It includes chiral-symmetry respecting and breaking pieces

Parametrization of transverse part of the vertex

- The tree-level vertex $\rho^{\mu}_{1,E} = (\delta^{\mu\nu} - \hat{k}^{\mu}_{E}\hat{k}^{\nu}_{E})\gamma^{\mu}_{E} \equiv \gamma^{\mu}_{T,E}$

  with $g_1(x) = 1 + \frac{1.67+0.204x}{1+0.683x+0.000851x^2}$

Parametrization of transverse part of the vertex

- Chiral-symmetry breaking structures ($s_E^\mu = (\delta^{\mu\nu} - \hat{k}_E^\mu \hat{k}_E^\nu)\bar{p}_E^\nu$)

$\rho^\mu_{2,E} = i\hat{s}^\mu_E$ and $\rho^\mu_{3,E} = i\hat{\not{k}}_E \gamma^\mu_{T,E}$

with $g_3(x) = -1.45 g_2(x) = \frac{0.365x}{0.0187+0.353x+x^2}$;

Parametrization of Landau-transverse part of the vertex

- The chirally symmetric structures

$$\rho^{\mu}_{4,E} = \hat{\not{k}}_E s^{\mu}_E \quad \text{and} \quad \rho^{\mu}_{7,E} = \hat{\not{s}}_E \hat{\not{k}}_E \gamma^{\mu}_{T,E}$$

$$\text{with} \quad g_4(x) = g_7(x) = \frac{2.59x}{0.859+3.27x+x^2} \; .$$

Extension to physical Minkowski space

First, the propagator mass function:

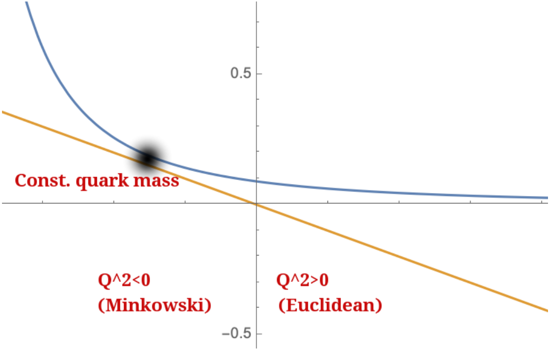

Euclidean q_E^2 functions (input from lattice, DSEs)

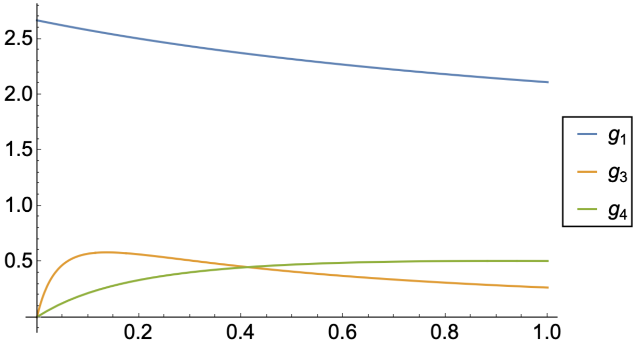

Next, the vertex dressing form factors:

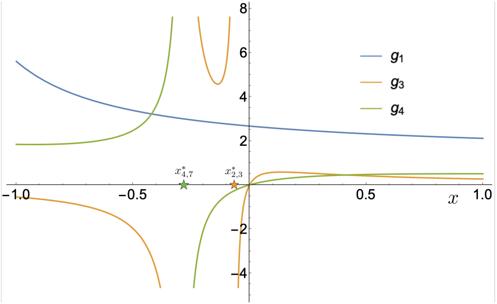

Note the $Q^2 < 0$ enhancement of the chiral symmetry breaking piece!

Breit-Wheeler process for $q\bar{q}$ creation

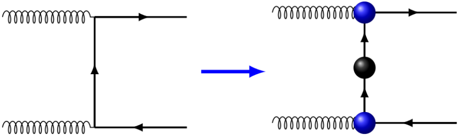

Breit-Wheeler process for $q\bar{q}$ creation

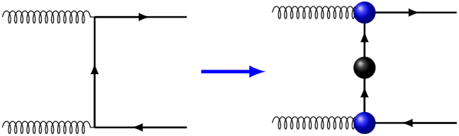

We couple flux-tube "gluons" to the quarks with the DSE functions

In a constant chromoelectric flux tube:

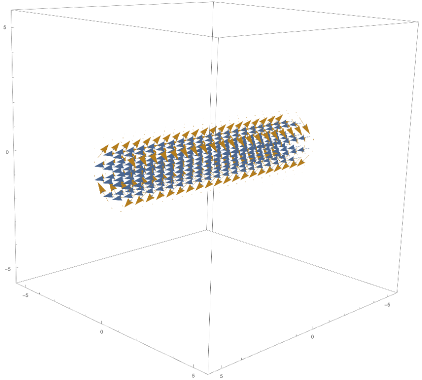

- Simplify to a constant chromo-E (parallel-plate capacitor)
  Background Landau-gauge field $(A_\rho, A_\theta, A_z, A_0) = (0, 0, 0, -Ez)$

In a constant chromoelectric flux tube:

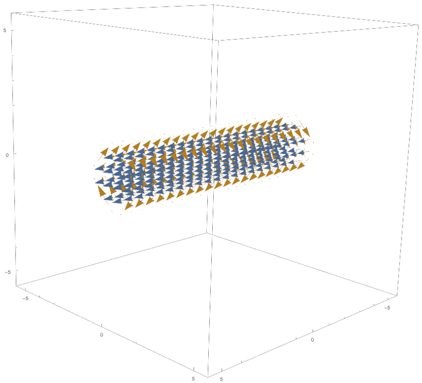

- Simplify to a constant chromo-E (parallel-plate capacitor)
  Background Landau-gauge field $(A_\rho, A_\theta, A_z, A_0) = (0, 0, 0, -Ez)$
- Think of the Schwinger pair-creation mechanism in QED.

In a constant chromoelectric flux tube:

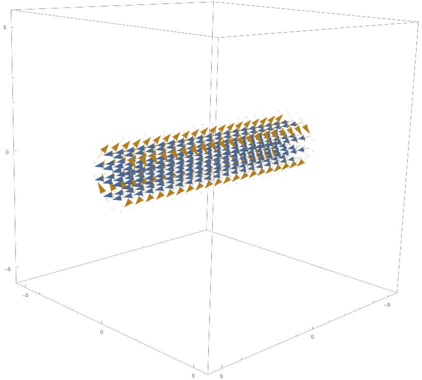

- Simplify to a constant chromo-E (parallel-plate capacitor)
  Background Landau-gauge field $(A_\rho, A_\theta, A_z, A_0) = (0, 0, 0, -Ez)$
- Think of the Schwinger pair-creation mechanism in QED.
- Rotation symmetry is broken: **must use notation for diatomic molecules!**. ${}^3P_0 \to {}^3\Pi_0$.

$$\langle \boldsymbol{p}s, \boldsymbol{q}s' | iT_{\text{singlet}} | 0\rangle =$$

$$\langle \boldsymbol{p}s, \boldsymbol{q}s' | -\frac{g^2}{2}\int d^4x \bar{\psi}_i(x) T^a_{ij} A^a_\mu(x) \Gamma^\mu \psi_j(x) \int d^4y \bar{\psi}_i(y) T^a_{ij} A^a_\nu(y) \Gamma^\nu \psi_j(y) |0\rangle =$$

$$= -g^2 \int d^4x d^4y \int \frac{d^4t}{(2\pi)^4} \tilde{A}^a_0(p-t)\tilde{A}^a_0(q+t)\mathcal{K}^{ss'}_{ab}(p,q,t)$$

where

$$\mathcal{K}^{ss'}_{ab}(p,q,t) \equiv \left[\bar{u}^s_i(p) T^a_{ij} \Gamma^0(p,-t) S(t) T^b_{jk} \Gamma^0(q,t) v^{s'}_k(q)\right]$$

and $S(t)$ is the dressed fermion propagator.

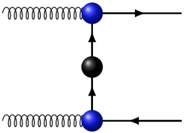

A relation between the gluon to quark kernel $\mathcal{K}$ and the pair production amplitude

$$\langle \boldsymbol{p}s, \boldsymbol{q}s' | iT_{\text{singlet}} | 0 \rangle = -(2\pi)^4 \delta^{(4)}(p+q)(gE)^2 \left[\frac{\partial}{\partial p^3} \frac{\partial}{\partial q^3} \mathcal{K}_{ab}^{ss'}(p,q,t) \right] \Big|_{t=-q}$$

- With the primitive Green's functions construct this skeleton kernel ✓
- Project it over ${}^{2S+1}L_J$ and numerically compare
  (But you can see that the chiral symmetry breaking part will be important, perhaps even dominant)

QED computation

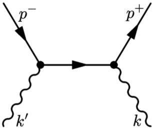

For a $(A_\rho, A_\theta, A_z, A_0) = (0, 0, 0, -Ez)$

$$(ie)^2 \frac{\partial}{\partial p^3} \frac{\partial}{\partial q^3} \left[\bar{u}^s(\boldsymbol{p}) \left(\gamma^0 - \frac{(\not{p}_+ - \not{t})}{p^0_+} \right) \frac{\not{t} + m}{t^2 - m^2} \left(\gamma^0 - \frac{(\not{p}_- + \not{t})}{p^0_-} \right) v^{s'}(\boldsymbol{q}) \right] \Big|_{\boldsymbol{t}=}$$

QED computation

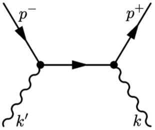

For a $(A_\rho, A_\theta, A_z, A_0) = (0,0,0,-Ez)$

$$(ie)^2 \frac{\partial}{\partial p^3}\frac{\partial}{\partial q^3}\left[\bar{u}^s(\boldsymbol{p})\left(\gamma^0 - \frac{(\not{p}_+ - \not{t})}{p^0_+}\right)\frac{\not{t}+m}{t^2-m^2}\left(\gamma^0 - \frac{(\not{p}_- + \not{t})}{p^0_-}\right)v^{s'}(\boldsymbol{q})\right]\Big|_{\boldsymbol{t}=}$$

This has a ${}^3P_0$ contribution:

$$\mathcal{A}^{^3\Sigma_1}_{\text{QED}}(|\boldsymbol{p}|) \propto -2\pi|\boldsymbol{p}|\left(\frac{E_{\boldsymbol{p}}-m}{E^4_{\boldsymbol{p}}}\right)$$

$$\mathcal{A}^{^3\Sigma_0}_{\text{QED}}(|\boldsymbol{p}|) = 0$$

$$\mathcal{A}^{^3\Pi_0}_{\text{QED}}(|\boldsymbol{p}|) \propto \frac{32m|\boldsymbol{p}|}{3E^4_{\boldsymbol{p}}}\,. \quad \Rightarrow \frac{\mathcal{A}^{^3\Pi_0}_{\text{QED}}}{\mathcal{A}^{^3\Sigma_1}_{\text{QED}}} = O\left(\frac{m^2}{|\mathbf{p}|^2}\right)$$

QED comparison of two field insertions

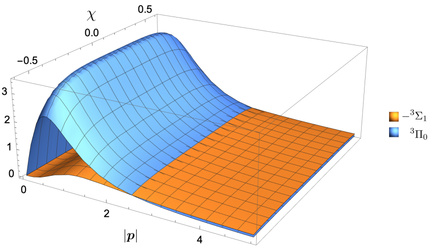

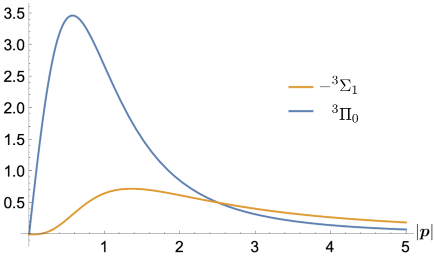

In QCD: two field insertions for getting the singlet

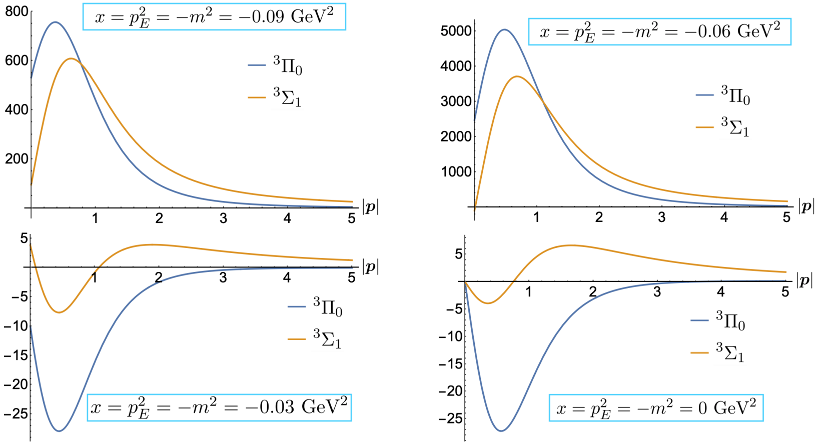

In QCD: two field insertions for getting the singlet

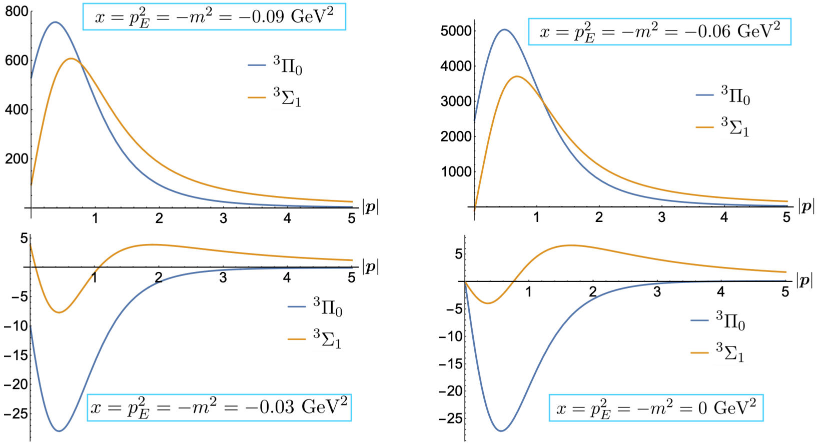

$^3\Sigma_1$ dominates at high momenta: spontaneous chiral symmetry breaking is less important.

In QCD: two field insertions for getting the singlet

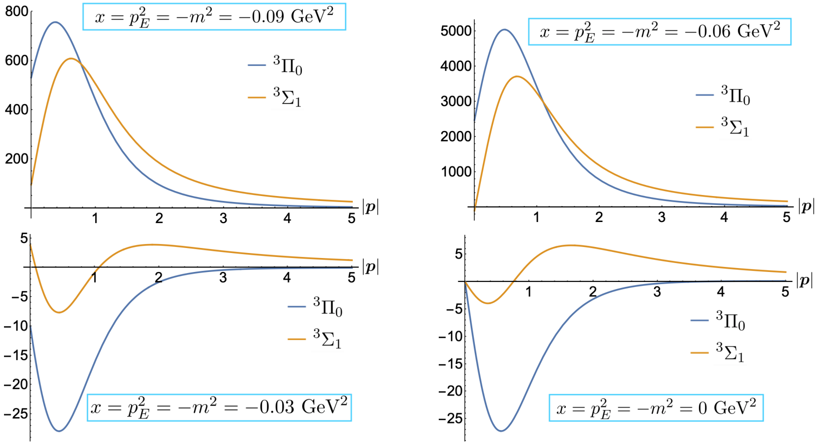

$^3\Sigma_1$ dominates at high momenta: spontaneous chiral symmetry breaking is less important. $^3P_0$ dominates at low momenta!

Threshold pair production comparison in Minkowski region

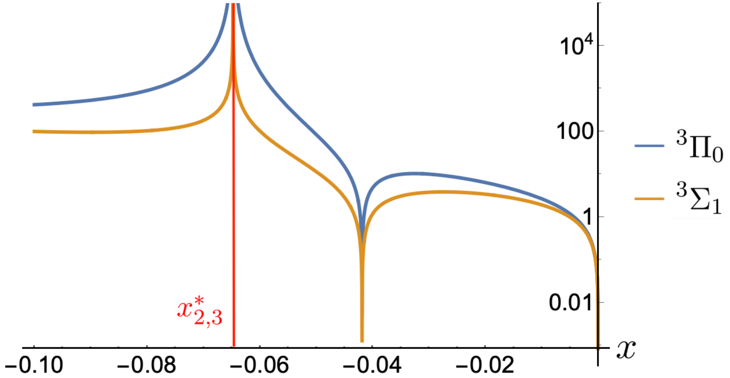

Threshold pair production comparison in Minkowski region

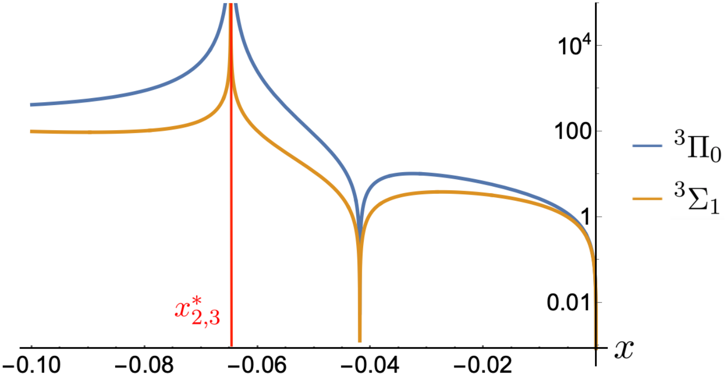

$^3P_0$ **Dominance at low momenta!**

Recap

- Historical $^3P_0$ mechanism of strong decays needs QCD grounding.

Recap

- Historical $^3P_0$ mechanism of strong decays needs QCD grounding.
- A first scan, clearly shows $^3\Pi_0$ dominance at lower momenta. Supporting quark-model lore for $^3P_0$ quark-antiquark pair creation for meson decays.

Recap

- Historical ${}^3P_0$ mechanism of strong decays needs QCD grounding.
- A first scan, clearly shows ${}^3\Pi_0$ dominance at lower momenta. Supporting quark-model lore for ${}^3P_0$ quark-antiquark pair creation for meson decays.
- Distinguishing ${}^3P_0$ from ${}^3\Pi_0$ may not be straightforward.

Recap

- Historical $^3P_0$ mechanism of strong decays needs QCD grounding.
- A first scan, clearly shows $^3\Pi_0$ dominance at lower momenta. Supporting quark-model lore for $^3P_0$ quark-antiquark pair creation for meson decays.
- Distinguishing $^3P_0$ from $^3\Pi_0$ may not be straightforward.
- Currently extending to open color decays of hybrid mesons (qqg).

Acknowledgments

Work of FJLE done as part of the Exotic Hadrons (ExoHad) Topical Coll. This project has received funding from the European Union's Horizon 2020 research and innovation programme under grant agreement No 824093; grants MICINN: PID2019-108655GB-I00, PID2019-106080GB-C21 (Spain); UCM research group 910309 and the IPARCOS institute. Funded by research grant PID2022-137003NB-I00 from spanish MCIN/AEI/10.13039/501100011033/ and EU FEDER.

Amplitudes 1

$$
\begin{aligned}
\mathcal{A}^{^3\Sigma_1}_{\mathrm{QCD}}(|\boldsymbol{p}|) \propto & \frac{-\pi}{E_{\boldsymbol{p}}^3\left(2E_B^2|\boldsymbol{p}|^4+\Lambda_B^4E_{\boldsymbol{p}}^2-|\boldsymbol{p}|^6\right)}\frac{E_B^2}{E_A^2}\Bigg(\\
& g_1^2\ 2|\boldsymbol{p}|E_{\boldsymbol{p}}\left[E_A^2m(Z_0-2)\Lambda_B^2+E_{AZ}^2\left(E_B^2E_{\boldsymbol{p}}+m|\boldsymbol{p}|^2\right)-m|\boldsymbol{p}|^2(Z_0-1)\Lambda_B^2\right] \\
& +g_2^2m|\boldsymbol{p}|E_{\boldsymbol{p}}\left[E_A^2\left(E_B^2(Z_0+1)-|\boldsymbol{p}|^2\right)-E_B^2|\boldsymbol{p}|^2(Z_0-1)\right] \\
& +g_3^2\ 2|\boldsymbol{p}|E_{\boldsymbol{p}}\left(2E_A^2\Lambda_B^2m+E_{AZ}^2E_B^2m+E_{AZ}^2E_B^2E_{\boldsymbol{p}}\right) \\
& +g_4^2m|\boldsymbol{p}|E_{\boldsymbol{p}}\left(E_A^2\Lambda_B^2-E_{AZ}^2E_B^2\right) \\
& +g_7^2\ 2m|\boldsymbol{p}|E_{\boldsymbol{p}}\left(-E_A^2\Lambda_B^2-2E_{AZ}^2E_B^2\right) \\
& +g_1g_2\ 2E_{\boldsymbol{p}}[\Lambda_A^2E_B^2|\boldsymbol{p}|^2Z_0+mE_A^2\Lambda_B^2(E_{\boldsymbol{p}}-m)+E_B^2|\boldsymbol{p}|^4] \\
& +g_1g_3\ 4|\boldsymbol{p}|E_{\boldsymbol{p}}E_{AZ}^2E_B^2\left(m+E_{\boldsymbol{p}}\right) \\
& +g_1g_7\ 2E_{\boldsymbol{p}}\left[E_A^2\left(m|\boldsymbol{p}|^2\left(m+3E_{\boldsymbol{p}}\right)-E_B^2\left(\left(m^2-|\boldsymbol{p}|^2Z_0\right)+3mE_{\boldsymbol{p}}\right)\right)-E_B^2|\boldsymbol{p}|^4(Z_0-1)\right] \\
& +g_3g_7\ 2E_{\boldsymbol{p}}\left(3E_A^2m|\boldsymbol{p}|^2(E_{\boldsymbol{p}}+m)+3E_{AZ}^2E_B^2|\boldsymbol{p}|^2-3E_A^2E_B^2m^2-mE_A^2E_B^2E_{\boldsymbol{p}}\right) \\
& +g_4g_7\ 2m|\boldsymbol{p}|E_{\boldsymbol{p}}\left(E_{AZ}^2E_B^2-E_A^2E_B^2+E_A^2|\boldsymbol{p}|^2\right) \\
& +g_2g_3\ 2\left(-E_A^2\Lambda_B^2m(E_{\boldsymbol{p}}-m)-\Lambda_A^2E_B^2|\boldsymbol{p}|^2Z_0-E_B^2|\boldsymbol{p}|^4\right) \\
& +2g_2g_7m|\boldsymbol{p}|E_{\boldsymbol{p}}\left(E_A^2\left(E_B^2(Z_0+1)-|\boldsymbol{p}|^2\right)-E_B^2|\boldsymbol{p}|^2(Z_0-1)\right)\Bigg)
\end{aligned}
\tag{1}
$$

Amplitudes 2

(2)

$$
\begin{aligned}
\mathcal{A}_{\rm QCD}^{^3\Pi_0}(|\boldsymbol{p}|) \propto & \frac{-16/3}{E_{\boldsymbol{p}}^2\left(-2E_B^2|\boldsymbol{p}|^4-\Lambda_B^4E_{\boldsymbol{p}}^2+|\boldsymbol{p}|^6\right)}\frac{E_B^2}{E_A^2}\Bigg(\\
& g_1^2\ m|\boldsymbol{p}|\left(E_A^2\left(E_B^2(Z_0-3)+3|\boldsymbol{p}|^2\right)-E_B^2|\boldsymbol{p}|^2(Z_0-1)\right) \\
& +g_2^2\ m|\boldsymbol{p}|\left(E_A^2\left(E_B^2(Z_0+1)-|\boldsymbol{p}|^2\right)-E_B^2|\boldsymbol{p}|^2(Z_0-1)\right) \\
& +g_3^2\ m|\boldsymbol{p}|\left(E_A^2\left(E_B^2(Z_0+3)-3|\boldsymbol{p}|^2\right)-E_B^2|\boldsymbol{p}|^2(Z_0-1)\right) \\
& +g_4^2\ m|\boldsymbol{p}|\left(E_B^2|\boldsymbol{p}|^2(Z_0-1)-E_A^2\left(E_B^2(Z_0-1)+|\boldsymbol{p}|^2\right)\right) \\
& -g_7^2\ m|\boldsymbol{p}|\left(E_A^2\left(3Z_0E_B^2+\Lambda_B^2\right)+3|\boldsymbol{p}|^2E_B^2(1-Z_0)\right) \\
& +g_1g_2\ 2\left(-m^2E_A^2\Lambda_B^2+|\boldsymbol{p}|^2\Lambda_A^2E_B^2Z_0+|\boldsymbol{p}|^4E_B^2\right) \\
& +g_1g_3\ 2|\boldsymbol{p}|E_{\boldsymbol{p}}E_{AZ}^2E_B^2 \\
& -g_1g_7\ 4mE_{\boldsymbol{p}}E_A^2\Lambda_B^2 \\
& -g_2g_3\ 2mE_{\boldsymbol{p}}E_A^2\Lambda_B^2 \\
& +g_3g_7\ 4\left(-m^2E_A^2\Lambda_B^2+|\boldsymbol{p}|^2\Lambda_A^2E_B^2Z_0+|\boldsymbol{p}|^4E_B^2)\right) \\
& +g_4g_7 2m|\boldsymbol{p}|\left(\Lambda_A^2E_B^2(Z_0-1)+|\boldsymbol{p}|^2E_A^2\right)\Bigg)\ . \qquad (3)
\end{aligned}
$$

$^3P_0$ vs. $^3\Pi_0$

Our finding lends support to the traditional $^3P_0$ mechanism in the following sense. Since $^3\Pi_0$ requires $m_L = 1 \implies L \geq 1$, without restricting total J, the smallest angular momenta (and thus the smallest energy required to overcome centrifugal barriers and chromomagnetic effects) is the $L = 1$, $J = 0$ configuration, or $^3P_0$. To distinguish $^3P_0$ and $^3\Pi_0$ does not seem possible with basic meson decays, interpreted as $(q\bar{q}) \to (q\bar{q})(q\bar{q})$.

To see this, note that for the parent meson, the possible quantum numbers are spin $s_i = 0, 1$, internal orbital angular momentum l, and parity $P_i = (-1)^{l+1}$. The two daughter mesons in the final state have $s_f = 0, 1, 2$, internal and relative orbital l_1, l_2, L and parity (one antiparticle has been produced) $P_f = (-1)^{l_1+l_2+L+2}$, meaning that orbital angular momentum has to change by an odd number of units to preserve parity.

Total angular momentum conservation implies that $\Delta J = 0$, so the changes in spin and orbital angular momentum have to compensate each other, $|\Delta S| = |\Delta L|$. Because $\Delta S = 0, \pm(1, 2)$, these are the values that ΔL can take. Among them, $\Delta L = 1$ is common to both $^3P_0$ and $^3\Pi_0$, $\Delta L = 0$ to none, and only $\Delta L = 2$ could distinguish the two mechanisms. But this is an even change in orbital angular momentum, which parity conservation does not allow. So it looks unpromising to try to distinguish both mechanisms, and they are for all purposes undistinguishable in ordinary mesons.

Chiral symmetry breaking

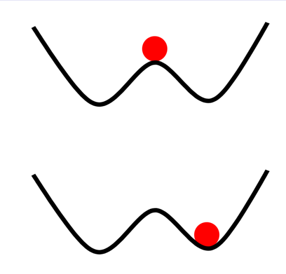

Chiral symmetry breaking

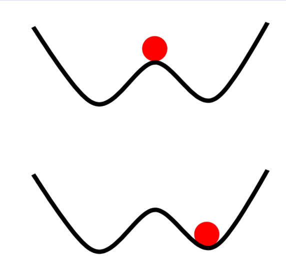

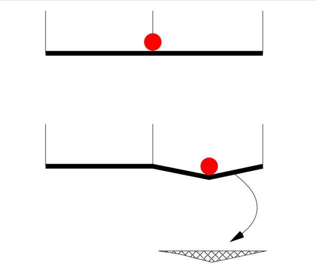

R. Alkofer *et al.* Annals Phys. **324** (2009) 106-172

Not very good rejection tests of $S = 1$ with light quarks

Famous selection rule: $A(S=0) \nrightarrow B(S=0) + C(S=0)$

(tests the "3" part of ${}^3P_0$)

Not very good rejection tests of $S = 1$ with light quarks

Famous selection rule: $A(S=0) \nrightarrow B(S=0) + C(S=0)$

(tests the "3" part of ${}^3P_0$)

List of $S = 0$ quantum numbers:

L	$J^{P(C)}$	
0	$0^{-(+)}$	π, η, K...
1	$1^{+(-)}$	h_1, b_1, ...
2	$2^{-(+)}$	π_2, η_2 ...
3	$3^{+(-)}$	h_3, b_3, ...
...		